

Antifouling and biodegradable poly(*N*-hydroxyethyl acrylamide) (polyHEAA)-based nanogels

Cite this: *RSC Adv.*, 2013, **3**, 19991

Chao Zhao,^a Kunal Patel,^b Lindsay Marie Aichinger,^a Zhaoqian Liu,^a Rundong Hu,^a Hong Chen,^a Xiaosi Li,^a Lingyan Li,^a Ge Zhang,^b Yung Chang^c and Jie Zheng^{*a}

We synthesize and characterize two types of poly(*N*-hydroxyethyl acrylamide) (polyHEAA)-based nanogels: antifouling poly(2-(methacryloyloxy) ethyl trimethyl ammonium-*g*-*N*-hydroxyethyl acrylamide) (polyTM-*g*-HEAA) by a new two-step polymerization method of inverse microemulsion ATRP and surface-initiated atom transfer radical polymerization (SI-ATRP), and pH-responsive biodegradable polyHEAA nanogels by the inverse microemulsion free radical polymerization method. PolyTM-*g*-HEAA nanogels with a core-shell structure by grafting antifouling polyHEAA onto the cationic polyTM core are tested for their antifouling property and stability in fetal bovine serum (FBS) and nanogels-induced cell toxicity. Results show that with the antifouling protection of polyHEAA, polyTM-*g*-HEAA nanogels significantly improve their long-term stability in FBS up to 7 days by preventing nonspecific protein adsorption, and they also improve cell viability to ~94% and exhibit almost neglectable cell toxicity. Further, polyHEAA nanogels cross-linked with acid-labile ethylidenebis(oxy-2,1-ethanediy) ester (EOE) are synthesized, which exhibit both biodegradation and control-release of encapsulated rhodamine 6G (R6G) at acid conditions. Conjugation of transferrin ligands onto R6G-loaded polyHEAA nanogels further enhances cellular uptake efficiency and intracellular drug release for targeting drug delivery. This work demonstrates that polyHEAA-based nanogels with easy synthesis, excellent antifouling property and stability, biodegradability, low toxicity, and pH-responsive intracellular drug release are highly promising for targeted drug delivery systems for biomedical applications.

Received 10th May 2013

Accepted 12th August 2013

DOI: 10.1039/c3ra42323a

www.rsc.org/advances

1. Introduction

Polymer-based nanodelivery systems offer many advantages for targeted drug/gene delivery in a controlled-release manner, which would have great potential to treat numerous diseases, including cancers.^{1,2} Because of a wide variety of polymers with different but tunable chemistries and structures, along with many different synthesis methods, the nanodelivery systems can be readily prepared with well-defined physical structures and sizes, tunable chemical compositions, and desirable functions.³⁻⁵ Additionally, these systems can also be conjugated with bioactive ligands to realize specific recognition of cell receptors for improving targeted delivery and reducing side effects. Significant progress has made in the development of polymer-based nanodelivery systems including polymer micelles, liposomes, hydrogels, nanoparticles, and nanogels.^{6,7} However, most of nanodelivery systems are still far from optimal for (pre)clinical applications. A number of limitations and challenges – including

short circulation time, low drug loading and uptake, poor stability before targeting and biodegradability after targeting, or any combination among them – have hindered the development of effective and biological benign nanodelivery systems.

To remedy the limitations for current nanodelivery systems, numerous strategies and techniques have been developed to improve the targeted delivery efficacy. First, many antifouling materials, which possess strong resistance to nonspecific protein adsorption known as the stealth effect,⁸⁻¹⁰ have been exclusively used as delivery carriers to increase blood circulation time, structural stability, and the solubility of many low soluble drugs.¹¹⁻¹³ However, even the most widely used poly(ethylene glycol) (PEG)-based drug delivery systems¹⁴⁻¹⁸ have often demonstrated *in vitro* instability, due to the oxidation and decomposition of ethylene units in most common biochemical solution containing transition-metal ions or in the presence of oxygen.^{19,20} Recently, zwitterionic-based water-soluble polymers such as sulfobetaine and carboxybetaine have demonstrated their long-term stability *in vitro* due to the super-low fouling properties.²¹⁻²⁴ Second, prodrug approaches using polymeric drug conjugates are often used to increase the higher drug loading capacity and to improve the targeted delivery of drugs to a specific location.²⁵ Furthermore, upon completion of drug release, the degradability of the nanodelivery systems are highly preferred to eliminate

^aDepartment of Chemical and Biomolecular Engineering, The University of Akron, Akron, Ohio, USA, 44325. E-mail: zhengj@uakron.edu

^bDepartment of Biomedical Engineering, The University of Akron, Akron, Ohio, USA, 44325

^cR&D Center for Membrane Technology and Department of Chemical Engineering Chung Yuan Christian University, Jhong-Li, Taoyuan 320, Taiwan

the need of surgery for removing residuals from human body, which will avoid any possible immune response and cytotoxic side effect. Biodegradable cross-linkers in polymer-based delivery systems in response to external stimuli such as temperature, pH, and light are often used for the sustained release of drugs over a prolonged period.^{26,27} All of these strategies have recently attracted significant attention for the development of effective polymer-based delivery systems for current drugs, which are equally important for the development of new drugs, which is a very time-consuming and costly procedure.^{27–29}

We have recently synthesized a series of poly(*N*-hydroxyethyl acrylamide) (polyHEAA)-based materials for different bio-applications. PolyHEAA brushes exhibited strong and long-term surface resistance to protein adsorption ($<0.3 \text{ ng cm}^{-2}$) from undiluted blood plasma and serum, as well as cell adhesion and bacterial colonization for up to 3 days.³⁰ PolyHEAA-coated gold nanoparticles (HEAA–AuNPs) also exhibited long-term super-low fouling ability and structural stability in undiluted human blood serum and plasma, without inducing any particle aggregation and protein adsorption up to 7 days.³⁰ Hybrid polyHEAA/salicylate hydrogels achieved both antifouling and antimicrobial activities.⁷ pH-sensitive poly(HEAA/acrylic acid) nanogels exhibited superlow fouling ability, ultrastability, low toxicity, and high cellular uptake for controlled release of drug *in vitro*.³¹ Similar to PEG-based materials, polyHEAA achieves its super-low fouling ability by forming a strong hydration layer around amide and hydroxyl groups, which create a high energy and physical barrier to prevent protein adsorption.

Encouraged by the excellent antifouling performance of polyHEAA materials, here we extended this successful super-low fouling polyHEAA to two polyHEAA-based nanogels – antifouling poly(2-(methacryloyloxy) ethyl trimethyl ammonium-*g*-*N*-hydroxyethyl acrylamide) (polyTM-*g*-HEAA) nanogels with a core-shell structure and pH-responsive biodegradable polyHEAA nanogels – to demonstrate that the introduction of HEAA as a protective antifouling sheath enables to greatly improve biocompatibility and stability, to reduce cell toxicity, and to realize cellular uptake efficacy and subsequent intracellular drug delivery. First, cationic polymers have been widely used as gene/drug delivery carriers,^{32,33} simply because the cationic polymers enable to interact strongly with most of anionic cell membrane to facilitate the transport of polymer carriers and drugs into intracellular targets. On the other hand, the cationic nature of the polymers also induce significant non-specific protein adsorption on the surface of cationic carriers, which will decrease the circulation time of carriers *in vivo* and block drug diffusion from carriers, and also induce high toxicity to normal human tissue cells.³⁴ To overcome such limitations, we develop a new two-step ATRP method to prepare polyTM-*g*-HEAA nanogels with a core-shell structure by grafting antifouling polyHEAA onto the surface of polyTM nanogels *via* SI-ATRP. The stability and toxicity of polyTM-*g*-HEAA nanogels were tested by dynamic light scattering (DLS) and live/dead SH-SY5Y cell assay, respectively. Further, we synthesize biodegradable and pH-responsive polyHEAA nanogels cross-linked with ethylenedibis(oxy-2,1-ethanediy) ester (EOE) and conjugated with transferrin ligands for cell targeting, in which HEAA serves as an excellent non-fouling background,

EOE cross-linker provides degradable sites at acid conditions, and transferrin is used for improving cellular uptake. The polyHEAA–EOE–transferrin nanogels combined these characteristics enable to retain large drug storage and high stability at neutral conditions, while degrading into small fragments to trigger intracellular drug release at acid conditions. Completion of this work, along with our previous works, will provide a complete framework for polyHEAA-based antifouling materials with different polymer architectures from polymer brushes, hydrogels, nanoparticles, to nanogels targeting for a wide range of applications of antifouling coating, wound dressing, and drug delivery.

2. Materials and methods

2.1. Materials

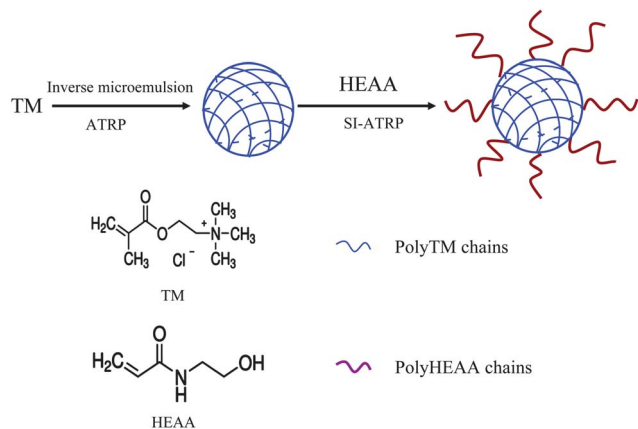
N-Hydroxyethyl acrylamide (HEAA, 97%), 1,1-dimethoxyethane (97%), 2-hydroxyethylacrylate (96%), *p*-toluenesulfonic acid monohydrate (*p*-TSA, 98.5%), acryloyl chloride (97%), 2,2'-bipyridyl (BPY, 99%), copper(i) bromide (99.999%), copper(i) chloride (CuCl, 99.999%), *N,N'*-methylene-bis-acrylamide (MBAA), ethylene bis(2-bromoisobutyrate) (97%), 2-(methacryloyloxy) ethyl trimethyl ammonium (TM, 80 wt% in H₂O), span 80, tween 80, rhodamine 6G (R6G, 99%), transferrin human (98%), *N,N'*-disuccinimidyl carbonate (DSC, 95%), 4-(dimethylamino)pyridine (DMAP, 99%), anhydrous *N,N*-dimethylformamide (DMF, 99.8%), benzene (anhydrous, 99.8%), hexane (95%), phosphate buffer saline (PBS, pH 7.4, 0.15 M, 138 mM NaCl, 2.7 mM KCl), ethanol (absolute 200 proof), tetrahydrofuran (THF HPLC), dichloromethane (99.9%), sodium hydroxide (NaOH, 99.99%), ethyl acetate (99.8%), and hydrochloric acid (HCl, 37%) were purchased from Sigma-Aldrich (Milwaukee, WI). Tris[2-(dimethylamino)ethyl]amine (Me₆TREN, 99%) was purchased from Alfa Aesar (Ward Hill, MA). Fetal bovine serum (FBS) was purchased from BioChemed Services (Winchester, VA). 2,2'-Azobis(4-methoxy-2,4-dimethyl valeronitrile) (V-70) was purchased from Wako Pure Chemical Industries (Osaka, Japan). Water used in these experiments was purified by a Millipore water purification system with a minimum resistivity of 18.0 MΩ cm.

2.2. Synthesis of ethylenedibis(oxy-2,1-ethanediy) ester (EOE) crosslinker

EOE was synthesized through transacetalization of 1,1-dimethoxyethane (2.4 g, 26 mmol) with 2-hydroxyethylacrylate (6.0 g, 52 mmol) in the presence of *p*-TSA catalyst (110 mg, 0.64 mmol) in dry benzene (200 mL) at room temperature for 2 h, then the methanol was continuously removed by distillation of the benzene-methanol azeotrope (58 °C) for 1 h. After the reaction, the solvent was removed by a rotary evaporation process, and the crude product was purified by flash column chromatography on silica gel with 3 : 1 hexane/ethyl acetate and finally with 1 : 1 hexane/ethyl acetate. The EOE crosslinker was obtained as a transparent liquid and was stored at –20 °C.

2.3. Preparation of nanogels

As shown in Scheme 1, polyTM-*g*-HEAA nanogels with core-shell structure were prepared by two-step polymerization



Scheme 1 Synthesis of polyTM-g-HEAA nanogel with a core-shell structure.

method. First, polyTM nanogels were prepared using an inverse microemulsion atom transfer radical polymerization (ATRP) method. A continuous-phase solution contained 40 mL of hexane, 1.4 g of tween 80, 1.6 g of span 80, and ethylene bis(2-bromoisobutyrate) (8 mg, 0.022 mmol). Aqueous monomer stock solution was prepared by dissolving TM (415 μ L, 1.8 mmol) and MBAA (18.4 mg, 0.12 mmol) in 2 mL of DI water. CuBr (14.3 mg, 0.1 mmol) and BPY (31.2 mg, 0.2 mmol) were placed in a reaction flask, followed by evacuation and nitrogen injection by three times. Degassed aqueous monomer stock solution was first added into the flask to dissolve the catalyst, and then the degassed continuous-phase solution was added into the flask, followed by vigorous shaking and sonication for 2 minutes. The reaction was maintained at room temperature with stirring and was protected under nitrogen for 4 hours. Second, SI-ATRP method was used to graft polyHEAA onto the surface of polyTM nanogels. CuCl (16.8 mg, 0.170 mmol) and 25 mg polyTM nanogel were placed in a reaction tube sealed with rubber septum stoppers and under nitrogen protection. Degassed ethanol (2 mL) was added to the tube. HEAA (1 g, 8.69 mmol) and Me₆TREN (40 mg, 0.174 mmol) were dissolved in Milli-Q water (5 mL) and ethanol (3 mL), and deoxygenated by passing a continuous stream of dry nitrogen through the solution while stirring. The solution with monomers was transferred to the tube using a syringe under nitrogen protection. The mixture was kept at room temperature with stirring and protected by dry nitrogen for 20 hours.

PolyHEAA nanogels were prepared by an inverse microemulsion free radical polymerization method as reported in our previous work.³¹ To synthesize polyHEAA nanogel, the continuous-phase solution contained 40 mL of hexane, 1.4 g of tween 80, 1.6 g of span 80, and V-70 (8 mg, 0.026 mmol). Aqueous monomer stock solution was prepared by dissolving HEAA (415 μ L, 4 mmol) of and EOE crosslinker (5 μ L, 0.02 mmol) into 2 mL of DI water. Then the aqueous stock solution was added to a 100 mL flask containing 40 mL of continuous-phase solution, followed by vigorous shaking and sonication for 2 minutes. The flasks were purged with nitrogen at 0 °C for 30 minutes to remove dissolved oxygen. During polymerization, the reaction was kept at 40 °C with stirring and was protected under nitrogen

for 4 hours. The same experimental conditions were used to synthesize polyHEAA nanogels with loaded R6G, by adding an additional R6G (4.79 mg, 0.01 mmol) to the aqueous stock solution.

After the polymerization, all nanogels were purified using the same method as follows: 30 mL of THF were added into the reaction solution and stirred for 1 h to remove surfactants. The mixture was centrifuged for 5 minutes at 8000 rpm. The supernatant was discarded, and the precipitate was washed with 30 mL of DI water. The final precipitate was stored at 4 °C for further characterization.

2.4. Characterization of nanogels

The hydrodynamic diameter and zeta potential of nanogels were evaluated by a Zetasizer Nano ZS dynamic light scattering (DLS) instrument (Malvern, U.K.). The wavelength of 633 nm and the scattering angle of 173° were fixed at room temperature. The dispersant refractive index and the viscosity of water were set to be 1.330 and 0.8872 cP, respectively. ¹H nuclear magnetic resonance (NMR) spectra were recorded using a Varian Mercury 300 MHz instruments, employing DMSO-*d*₆ (dimethylsulfoxide) as solvents.

2.5. Release of encapsulated drug from polyHEAA nanogels

40 milligrams of the purified nanogels with R6G drugs was re-suspended in 20 mL of buffer solution (stock solution) and left at 37 °C. Then, 1 mL of solution was taken from the nanogel solution. Considering that the R6G drugs that are loaded inside the nanogels and released in the solution can generate UV absorption signal. At $t = 0$, almost all of R6G were entrapped inside the nanogels after numerous washing with water. The initial UV density of the stock solution actually represents a total amount of R6G inside the nanogels. After that, the R6G drugs will be released from the nanogels into the solution. At different time points, 1 mL of solution was taken from the stock solution, placed into a 3 kDa molecular-weight-cutoff Amicon Ultra centrifugal filter device (Millipore, Burlington, MA), and centrifuged at 14 000 rpm for 30 minutes to collect flow-through solution for drug detection. The UV-vis density of R6G in the filtrate solution was measured by a Beckman model DU 530 spectrometer with cuvettes of 1 or 0.5 cm path length at room temperature. The percentage of released drugs was defined as the ratio of the UV-vis density of flow-through solution at different time points to the initial UV-vis density of stock solution

$$\text{Drug release (\%)} = \frac{\text{UV density}_{\text{flow-through solution}}}{\text{UV density}_{\text{stock solution}}} \times 100\%.$$

Different amounts of HCl were added into PBS buffer (pH = 7.4) to prepare the buffers with pH 1.6 and 3.6.

2.6. Conjugation of transferrin to the surface of polyHEAA nanogels

To activate the terminated hydroxyl groups of polyHEAA nanogels, 20 mg polyHEAA nanogels were dispersed in dry DMF solution containing 0.1 M DSC and 0.1 M DMAP for 24 h at room temperature under an argon atmosphere. After the

reaction, the reaction solution was centrifuged for 30 minutes at 14 000 rpm, and 10 mg precipitate was mixed with 500 μL aqueous solution of transferrin (10 mg mL^{-1}). The reaction was kept at room temperature with stirring for 24 h. After the reaction, the reaction solution was centrifuged for 30 minutes at 14 000 rpm, and the precipitates were collected for cell uptake assay.

2.7. Cell culture

All chemicals were purchased from Life Technologies unless otherwise stated. Human neuroblastoma (SH-SY5Y) cells (ATCC) were used as model neurons, and cultured in 75 cm^2 T-flasks (Corning) in sterile-filtered Eagle's Minimum Essential Medium and Ham's F-12 medium mixed at a 1 : 1 ratio containing 10% fetal bovine serum, and 1% penicillin/streptomycin. Flasks were incubated in a humidified 37 $^{\circ}\text{C}$ incubator with 5% CO_2 . Cells were cultured to confluence, and harvested using 0.25 mg mL^{-1} Trypsin/EDTA solution (Lonza). Cells were re-suspended in Opti-MEM reduced serum medium and counted using a hemacytometer. Cells were then placed in a 24-well tissue culture plate with approximately 100 000 cells per well in 500 μL of medium, which allow cells to attach for 24 hours inside the incubator.

2.8. Live/dead cell assay for polyTM-g-HEAA nanogels

A live/dead assay was used to obtain cell viability/cytotoxicity data and to observe live and dead cells. 0.25 mg of polyTM and polyTM-g-HEAA nanogels were added to each well and pipetted up and down a few times. The cells were then left for 24 hours in a humidified incubator with 5% CO_2 at 37 $^{\circ}\text{C}$, followed by the assessment of cell toxicity. Calcein AM was added to each well to a final concentration of 2 μM to distinguish the presence of live cells with a fluorescence excitation/emission of 494/517 nm, while ethidium homodimer-1 was added to each well to a final concentration of 5 μM to distinguish the presence of dead cells with a fluorescence excitation/emission of 528/617 nm. After being incubated for 15 min to activate the fluorescent dyes at room temperature, the fluorescence images of the live and dead cells was collected using a Zeiss Axiovert 40 CFL inverted microscope fitted with filters at 510 nm and 600 nm. Cell viability percentages were calculated using a Synergy H1 microplate reader (BioTek) with background subtraction. For cytotoxicity assay, six independent values were collected and the error bars in each figure represent the standard error of these six independent experiments. A result was considered statistically significantly different when $p \leq 0.05$.

2.9. Cell uptake assay for polyHEAA nanogels

R6G-loaded polyHEAA nanogels (0.05 mg and 0.1 mg) with or without transferrin conjugation were added to each well, respectively, and pipetted up and down a few times. Cells were incubated for 24 h. After washing the coverlips 3 times with 10 mM PBS, the cells were fixed with 3–4% paraformaldehyde, followed by 3 washes with PBS. The cells were examined under 20 \times magnifications through differential interference contrast and epifluorescence.

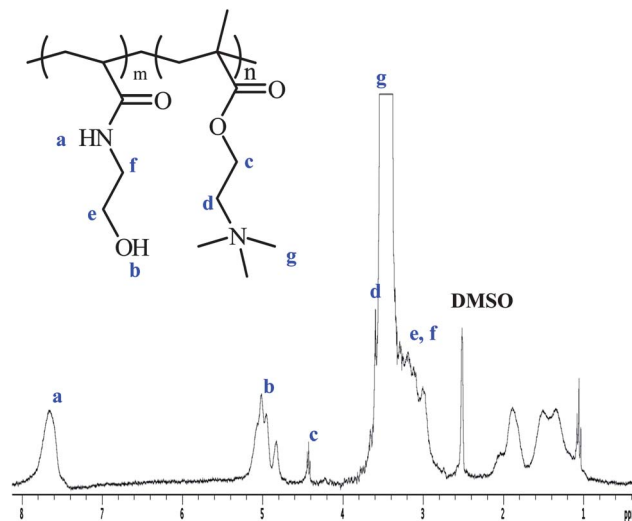


Fig. 1 ^1H NMR spectrum of polyTM-g-HEAA nanogels.

3. Results and discussion

3.1. Synthesis and characterization of antifouling polyTM-g-HEAA core-shell nanogels

PolyTM-g-HEAA core-shell nanogels were prepared *via* a new two-step ATRP method: cationic polyTM cores were first prepared *via* the inverse microemulsion ATRP, followed by the grafting of polyHEAA onto the surface of polyTM nanogels *via* the surface-initiated-ATRP method (Scheme 1). ^1H NMR was used to confirm the chemical structure of polyTM-g-HEAA nanogels. The chemical shifts of all the protons in the copolymers can be clearly identified in Fig. 1. Specifically, the chemical shifts in the region of 3.3–3.5 ppm (peak g) were assigned to the protons of $-\text{N}^+(\text{CH}_3)_3$ group of TM segment. The apparent signals at ~ 7.6 – 7.8 ppm (peak a) and 5.0–5.1 ppm (peak b) were characteristic peaks of the protons of $-\text{CO}-\text{NH}-$ group and $-\text{OH}$ group of HEAA segment, respectively. Copolymer compositions were also determined from the ^1H NMR by comparing the peak areas corresponding to the protons of $-\text{N}^+(\text{CH}_3)_3$ group at 3.3–3.5 ppm and the protons of $-\text{CO}-\text{NH}-$ group at 7.6–7.8 ppm. The mole ratio of TM *vs.* HEAA in polyTM-g-HEAA nanogels was estimated as $\sim 1 : 2.5$, while the molar ratio of MBAA to HEAA in the polyTM-g-HEAA nanogel was estimated as $\sim 2.7\%$. We should note that in the second SI-ATRP step, a large amount of HEAA was used to ensure the saturated grafting polymerization occurred on the surface of polyTM cores, but only a small percentage of HEAA monomers can be grafted on the polyTM surfaces. This is the interpretation for the low conversion of HEAA monomers between the large excess use of HEAA to TM for preparing the polyTM-g-HEAA nanogels and the small ratio of HEAA to TM (2.5 : 1) in the resulting polyTM-g-HEAA.

To verify whether the grafted polyHEAA shell provides antifouling protection to the polyTM core, the average hydrodynamic diameters of nanogels in the absence and presence of polyHEAA shell in fetal bovine serum (FBS) was determined and compared by DLS. Fig. 2 clearly showed that polyTM-g-HEAA nanogels were able to retain their initial hydrodynamic

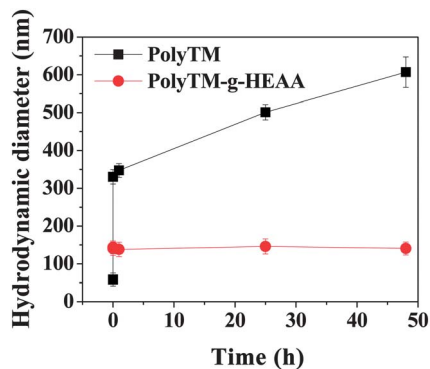


Fig. 2 Time-dependent hydrodynamic diameter of polyTM nanogels and polyTM-g-HEAA nanogels in FBS. Error bars represent standard deviation from 3 independent measurements.

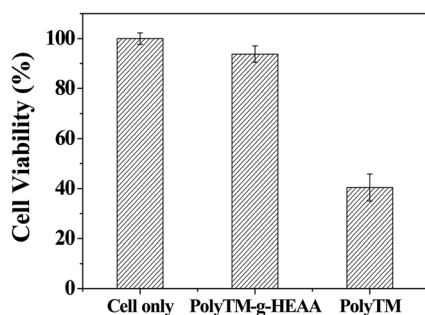


Fig. 3 Viability of SH-SY5Y cells following 24 h incubation with polyTM-g-HEAA and polyTM nanogels (0.5 mg mL^{-1}), as normalized by cell viability in medium only. Error bars represent standard deviation from 3 independent measurements.

diameters at 140 nm. The barely changed sizes of polyHEAA nanogels indicate that HEAA groups can effectively prevent both nonspecific protein adsorption on the nanogels and the self-aggregation of nanogels, resulting in more homogeneously dispersed and stable nanogels without aggregation in FBS over a long period time (up to 48 h). Conversely, cationic polyTM nanogels quickly increased their initial size from 58 nm to 330 nm within the first 5 min and then continuously increased to 607 nm after 48 h incubation in blood plasma. Such dramatic size increase is likely attributed to (i) the nonspecific adsorption of proteins from blood plasma onto the nanogels and (ii) the

self-aggregation of nanogels. The latter event should occur after the nonspecific adsorption of proteins. PolyTM nanogels themselves actually can remain their sizes unchanged in PBS for very long time, but upon the addition of plasma or serum, nonspecific protein adsorption on the surface of polyTM nanogel will further trigger the self-aggregation of the nanogels *via* nonspecific protein interactions. Meanwhile, the increase of initial hydrodynamic diameter from 58 nm for polyTM nanogels to 140 nm for polyTM-g-HEAA nanogel in FBS also indicates the successful graft of polyHEAA onto the polyTM nanogel. Clearly, the incorporation of polyHEAA onto the polyTM core confirms antifouling protection effect.

Since most of synthetical nanogels are often cytotoxic, we further evaluated the cytotoxicity of polyTM-g-HEAA nanogels using the live/dead SH-SY5Y cell assay as compared to pure polyTM nanogels without polyHEAA protection. After 24-hour incubation of SH-SY5Y cells with different nanogels, live and dead cells were quantitatively measured using a Synergy H1 microplate reader (Fig. 3) and qualitatively imaged using fluorescence microscopy (Fig. 4). With nanogel concentration of 0.5 mg mL^{-1} , cationic polyTM nanogels were highly toxic to cells and induced $\sim 60\%$ cell death, as compared to 98% cell viability in the absence of nanogels as a control. Conversely, polyTM-g-HEAA nanogels retained $\sim 94\%$ relative cell viability and exhibited almost neglectable cell toxicity. Meanwhile, visual inspection of live and dead cells using fluorescence microscopy also confirmed few cell death induced by polyTM-g-HEAA nanogels (Fig. 4b), as compared to massive cell death induced by polyTM nanogels (Fig. 4c). High instability and toxicity of polyTM nanogels are very likely attributed to their cationic surfaces. Strong electrostatic interactions between positively charged nanogels and negatively charged proteins in FBS and cell membranes would cause strong protein adsorption on the gel surfaces and strong membrane-binding and membrane disruption, respectively. As expected, Fig. 5 showed that ξ potentials of the polyTM nanogels in PBS were +30 mV, indicating that the polyTM nanogels carrying strong positive charges. While after grafting polyHEAA onto polyTM nanogels, the ξ potentials of polyTM-g-HEAA nanogels decreased to +3 mV, indicating the very weak surface charges. Taken together, incorporation of antifouling HEAA groups into the cationic core of polyTM nanogels significantly improves the biocompatibility, stability, and cell viability of nanogels.

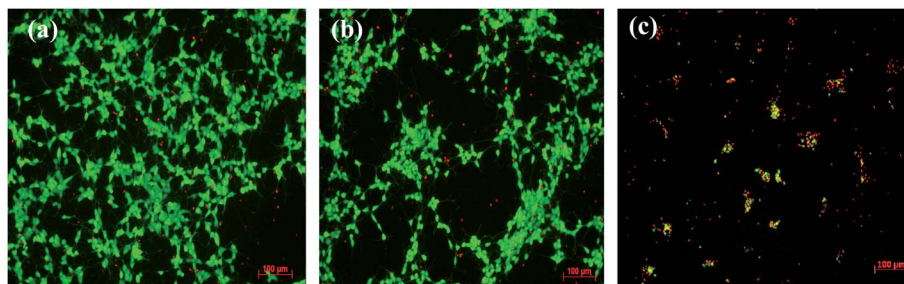


Fig. 4 Representative fluorescence microscopy images of SH-SY5Y cells after 24 h incubation with (a) medium only, (b) polyTM-g-HEAA nanogels (0.5 mg mL^{-1}), and (c) polyTM nanogels (0.5 mg mL^{-1}). Live cells are stained green, while dead cells are stained red.

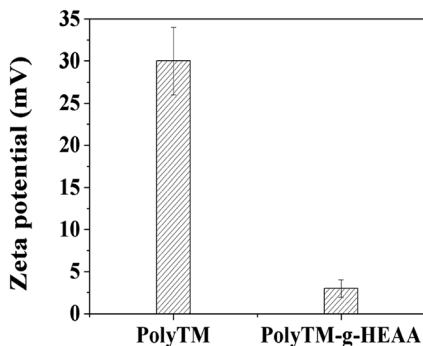


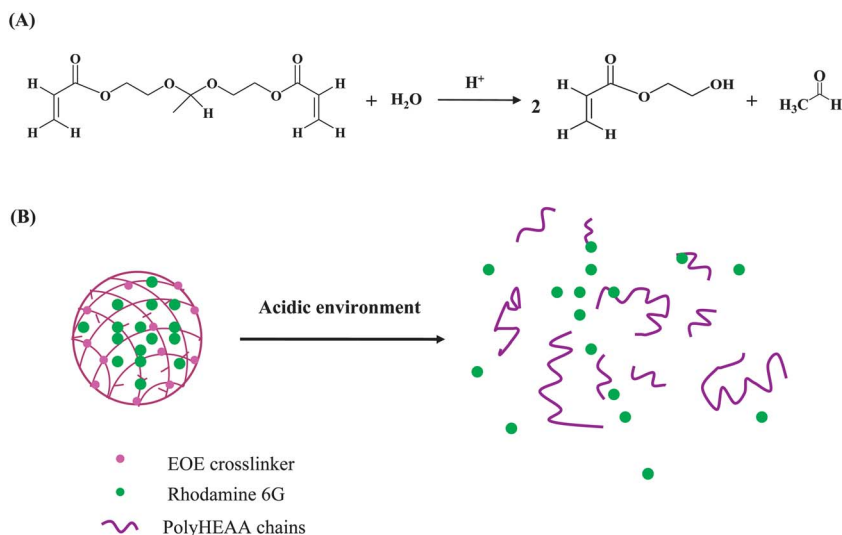
Fig. 5 Zeta potential of polyTM and polyTM-g-HEAA nanogels in PBS buffer (pH = 7.4). Error bars represent standard deviation from 3 independent measurements.

3.2. Synthesis and characterization of biodegradable polyHEAA nanogels

Besides the biocompatibility of nanogels, biodegradability is another important factor for their biomedical uses. Here, we prepared biodegradable polyHEAA nanogels cross-linked with 0.5% EOE *via* an inverse microemulsion free radical polymerization method. EOE as a degradable crosslinker is stable under neutral and alkaline conditions, however it readily undergoes hydrolysis in aqueous acidic solutions³⁵ (Scheme 2A). It is widely accepted that the intracellular pH of tumors is more acidic (pH 4.0–5.5) than that of blood and normal tissues. Therefore, the pH-responsive materials, such as EOE used in this work, offer a general advantage for drug release and cancer therapies, as compared to many other stimuli-responsive materials. The degradability of polyHEAA nanogels was determined by monitoring the hydrodynamic diameter of nanogels in PBS solutions of different pH values. As shown in Fig. 6, polyHEAA nanogels had initial average hydrodynamic diameter of ~130 nm (Fig. 6a). After incubating nanogels in PBS solutions with pH 1.6, 3.6, and 7.4 after 120 h, average diameters of

polyHEAA nanogels decreased to 10 nm, 18 nm, and 110 nm, respectively (Fig. 6b–d), indicating that nanogels indeed degrade. Further, a drastic decrease in gel sizes particularly at acid conditions suggests an accelerated hydrolysis leading to a faster degradation, while a slow degradation at neutral pH by only 15% actually indicates relative stability of polyHEAA nanogels against hydrolysis.

The degradation behavior of polyHEAA nanogels is not only tunable by varying the pH values, but also used to regulate drug release from the polyHEAA nanogels after uptake by cells. The acid-triggered release of drugs from polyHEAA nanogels cross-linked with 0.5% EOE was investigated. Positively charged R6G was used as model drug. To qualify the amount of R6G released from nanogels to aqueous solution, the concentration of released R6G was measured by UV-vis density at 25 °C. Fig. 7 shows the acidic-responsive release kinetics of R6G from polyHEAA nanogels cross-linked with EOE in PBS solutions with different pH. It can be seen clearly that at a strong acid condition of pH = 1.6, a relative fast drug-release from nanogels within 25 h was observed, in which *ca.* 2.0%, 16.2%, 34.2% drugs were released in 5, 10, 25 h, respectively. Similar drug-release trend was also observed but to a smaller extent at pH of 3.6. In contrast, minimal drug release (*ca.* 7.5%) was observed within 120 h at pH 7.4 under otherwise the same conditions. Overall, the cumulative percentages of released drugs after 120 h were 70% at pH 1.6, 45% at pH 3.6, and 7.5% at pH 7.4, respectively, further confirming that this acid-triggered drug release behavior is likely due to the degradability of a large fraction of nanogels at acid conditions, while still retaining a relative large drug storage and high stability of polyHEAA nanogels at physiological condition (Scheme 2B). Overall, the more acid condition, the higher degree of nanogel degradation, the more drug release percentage, explaining the fact that saturated drug release is in the order of pH values: 70% at pH = 1.6, 40% at pH = 3.6, and 7.5% at pH = 7.4. The biodegradable polyHEAA nanogels with easy synthesis, enhanced antifouling



Scheme 2 (A) Hydrolysis of an EOE crosslinker and (B) acid-triggered degradation of polyHEAA nanogel and subsequent R6G release from degraded nanogels.

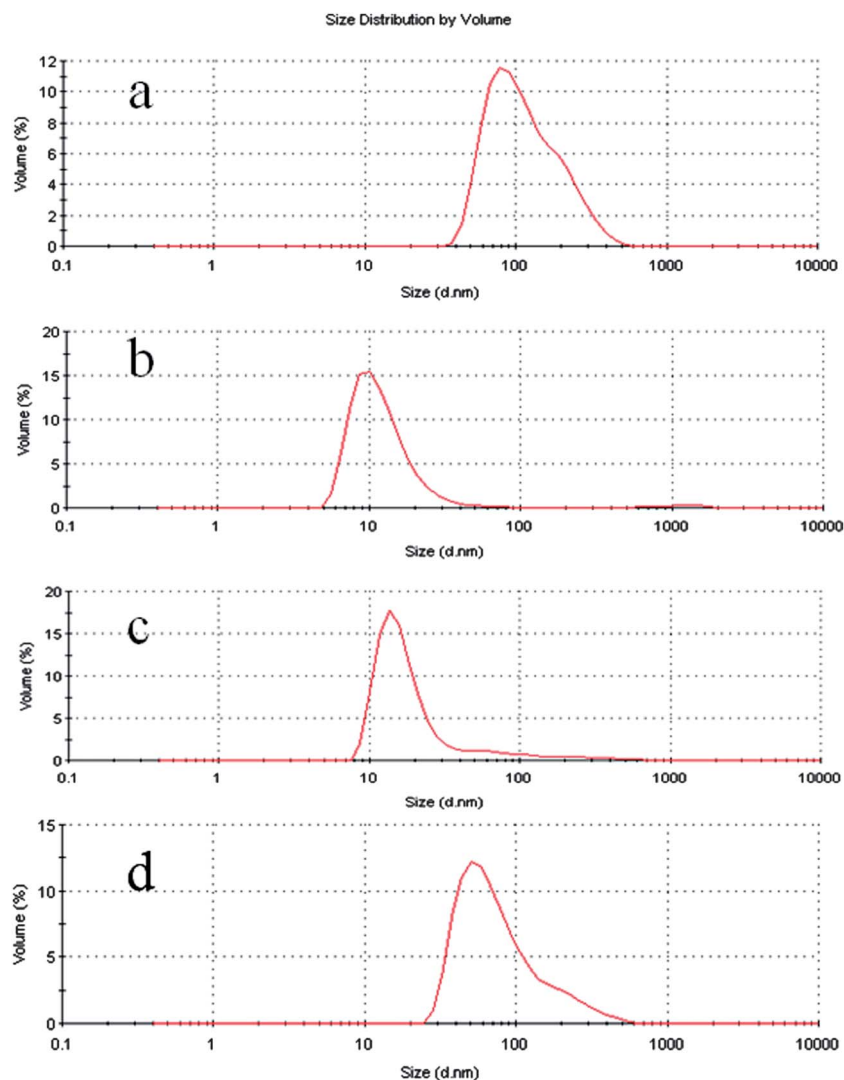


Fig. 6 Hydrodynamic diameter distributions of polyHEAA nanogels conjugated with EOE crosslinkers (a) before hydrolysis (initial diameters) and after hydrolysis when incubating nanogels in PBS solutions at (b) pH = 1.6, (c) pH = 3.6, and (d) pH = 7.4 for 120 h at 37 °C.

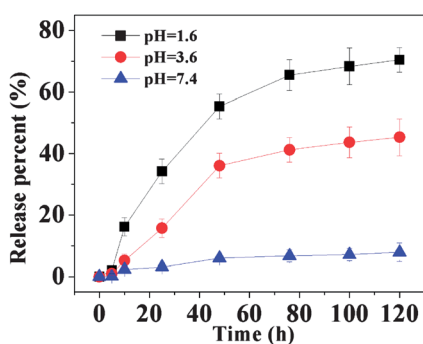


Fig. 7 Time-dependent release profiles of R6G from degradable polyHEAA nanogels in PBS solution of different pH values at 37 °C. Error bars represent standard deviation from 3 independent measurements.

ability and stability, and pH-triggered drug release behaviors are highly interesting as “smart” vehicles for active intracellular drug release.

Our previous live/dead assays have revealed that polyHEAA nanogels were nontoxic to SH-SY5Y cells with cell viabilities 93.4% up to a tested concentration of 0.5 mg mL⁻¹. Here, we extended the study to examine the SH-SY5Y cellular uptake and subsequent intracellular drug release behaviors of R6G-loaded polyHEAA nanogels with biodegradable cross-linkers. To realize efficient and specific intracellular drug delivery to tumor cells, we conjugated transferrin ligands onto the surface of polyHEAA nanogels using an activation-coupling approach, *i.e.* the hydroxyl groups of HEAA monomers are first activated with *N,N'*-disuccinimidyl carbonate, followed by subsequent coupling to a primary amine of transferrin. Transferrin, an iron-binding glycoprotein, is a well-studied ligand that facilitates efficient and specific tumor cell uptake of nanodelivery systems *via* receptor-mediated endocytosis. Fig. 8 compares differential interference contrast (left), the corresponding epifluorescent images (middle), and the merged images (right) of SH-SY5Y cells after 24 h incubation with R6G-loaded polyHEAA nanogels with and without conjugated transferrin. In all concentrations

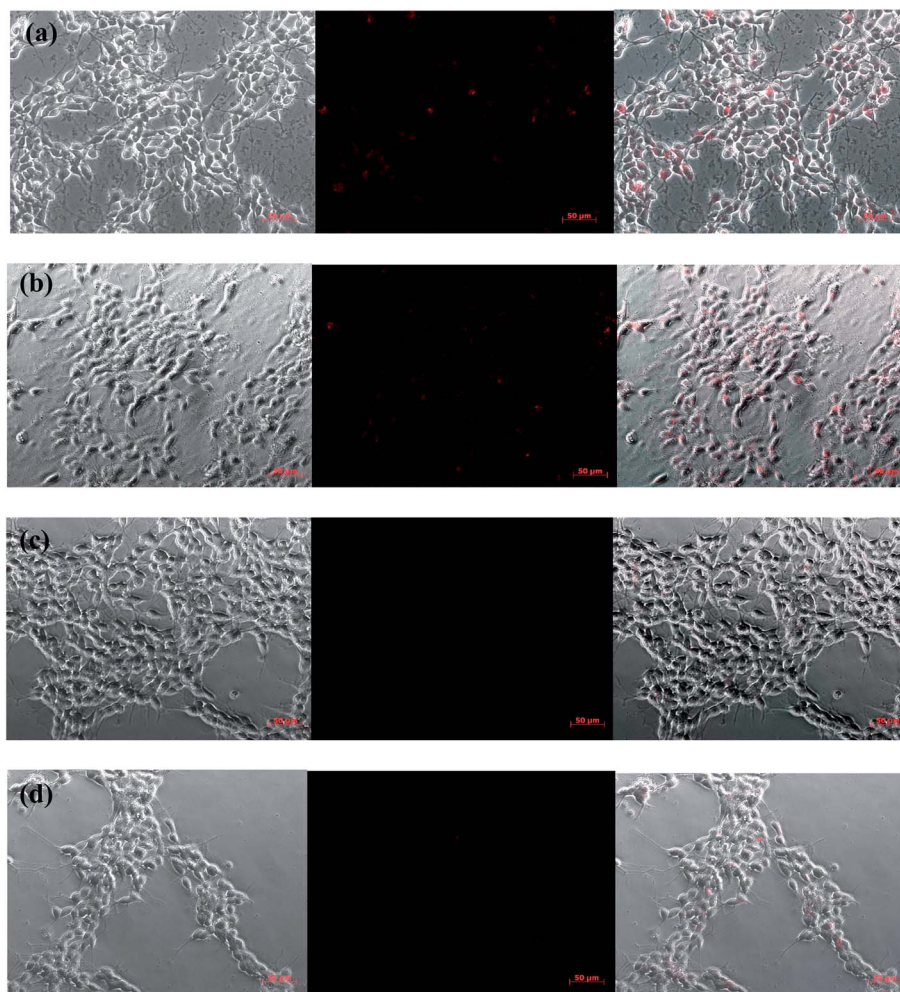


Fig. 8 Differential interference contrast images (left panel), epifluorescent images of rhodamine 6G (color in red) (middle panel), and merged images (right panel) of SH-SY5Y cells after 24 h incubation with (a) 0.1 mg mL^{-1} and (b) 0.2 mg mL^{-1} of R6G-loaded polyHEAA nanogels with transferrin, (c) 0.1 mg mL^{-1} and (d) 0.2 mg mL^{-1} of R6G-loaded polyHEAA nanogels without transferrin. The scale bars correspond to $50 \mu\text{m}$ in all the images.

tested, cells treated with R6G-loaded polyHEAA nanogels without conjugated transferrins displayed weak fluorescence (Fig. 8c–d). In contrast, upon conjugation with transferrin onto R6G-loaded polyHEAA nanogels, very bright fluorescence arising from R6G was observed in SH-SY5Y cells, indicating the internalization of nanogels and the release of drugs inside cells. After nanogels cellular uptake and drug releases, we did not observe apparent cell death, further confirming that these biodegradable nanogels have excellent biocompatibility. Overall, polyHEAA nanogels with excellent antifouling property, biodegradability, low toxicity, and pH-responsive intracellular drug release are highly promising for targeted cancer therapy.

4. Conclusions

This study has made a proof of concept that HEAA-functionalized polymers can be prepared for the construction of anti-fouling graft copolymer nanogels and pH-responsive biodegradable nanogels for different biomedical applications. Upon grafting of an antifouling polyHEAA shell to the polyTM

core, which switches positively charged gel surface to a neutral and hydrophilic surface, polyTM-*g*-HEAA nanogels dramatically improve their long-term stability in FBS and reduce toxicity to SH-SY5Y cells. Further, biodegradable polyHEAA nanogels cross-linked with acid-responsive EOE also exhibit fast degradation upon hydrolysis and drug release at acid conditions, while retaining relative large drug storage and high stability at physiological condition. Conjugation of transferrin onto polyHEAA nanogels further improves the efficiency of cellular uptake and subsequent intracellular drug release for targeting drug delivery. Overall, these HEAA-based nanogels exhibit excellent biocompatibility, enhanced stability, low cell toxicity, and pH-triggered degradability and intracellular drug release, which make them as great potential nanodelivery systems to be widely used in biomedical applications.

Acknowledgements

J.Z. thanks the support from NSF grants (CAREER Award CBET-0952624 and CBET-1158447).

References

- 1 D. Putnam, C. A. Gentry, D. W. Pack and R. Langer, Polymer-based gene delivery with low cytotoxicity by a unique balance of side-chain termini, *Proc. Natl. Acad. Sci. U. S. A.*, 2001, **98**, 1200–1205.
- 2 D. M. Lynn, M. M. Amiji and R. Langer, pH-responsive polymer microspheres: Rapid release of encapsulated material within the range of intracellular pH, *Angew. Chem., Int. Ed.*, 2001, **40**, 1707–1710.
- 3 S. P. Hudson, R. Langer, G. R. Fink and D. S. Kohane, Injectable *in situ* cross-linking hydrogels for local antifungal therapy, *Biomaterials*, 2010, **31**, 1444–1452.
- 4 D. N. Nguyen, J. J. Green, J. M. Chan, R. Longer and D. G. Anderson, Polymeric Materials for Gene Delivery and DNA Vaccination, *Adv. Mater.*, 2009, **21**, 847–867.
- 5 K. E. Uhrich, S. E. M. Ibim, D. R. Larrier, R. Langer and C. T. Laurencin, Chemical changes during *in vivo* degradation of poly(anhydride-imide) matrices, *Biomaterials*, 1998, **19**, 2045–2050.
- 6 X. Wang, X. Sun, G. Jiang, R. Wang, R. Hu, X. Xi, *et al.* Synthesis of biomimetic hyperbranched zwitterionic polymers as targeting drug delivery carriers, *J. Appl. Polym. Sci.*, 2013, **128**, 3289–3294.
- 7 C. Zhao, X. Li, L. Li, G. Cheng, X. Gong and J. Zheng, Dual functionality of antimicrobial and antifouling of poly(*N*-hydroxyethylacrylamide)/salicylate hydrogels, *Langmuir*, 2013, **29**, 1517–1524.
- 8 K. Knop, R. Hoogenboom, D. Fischer and U. S. Schubert, Poly(ethylene glycol) in Drug Delivery: Pros and Cons as Well as Potential Alternatives, *Angew. Chem., Int. Ed.*, 2010, **49**, 6288–6308.
- 9 S. Chen, L. Li, C. Zhao and J. Zheng, Surface hydration: principles and applications toward low-fouling/nonfouling biomaterials, *Polymer*, 2010, **51**, 5283–5293.
- 10 Y. Chang, W. Yandi, W.-Y. Chen, Y.-J. Shih, C.-C. Yang, Y. Chang, *et al.* Tunable bioadhesive copolymer hydrogels of thermoresponsive poly(*N*-isopropyl acrylamide) containing zwitterionic polysulfobetaine, *Biomacromolecules*, 2010, **11**, 1101–1110.
- 11 C. Zhao, L. Li and J. Zheng, Achieving highly effective nonfouling performance for surface-grafted poly(HPMA) *via* atom-transfer radical polymerization, *Langmuir*, 2010, **26**, 17375–17382.
- 12 C. Zhao, L.-Y. Li, M.-M. Guo and J. Zheng, Functional polymer thin films designed for antifouling materials and biosensors, *Chem. Pap.*, 2012, **66**, 323–339.
- 13 C. Zhao, L. Li, Q. Wang, Q. Yu and J. Zheng, Effect of film thickness on the antifouling performance of poly(hydroxy-functional methacrylates) grafted surfaces, *Langmuir*, 2011, **27**, 4906–4913.
- 14 V. Zoulalian, S. Zürcher, S. Tosatti, M. Textor, S. Monge and J.-J. Robin, Self-Assembly of Poly(ethylene glycol)-Poly(alkyl phosphonate) Terpolymers on Titanium Oxide Surfaces: Synthesis, Interface Characterization, Investigation of Nonfouling Properties, and Long-Term Stability, *Langmuir*, 2009, **26**, 74–82.
- 15 H. Otsuka, T. Satomi, K. Ueno, Y. Mitamura and T. Tateishi, Synthesis of polypyridine-graft-PEG copolymer for long-term stability of nonfouling character, in *Transactions of the Materials Research Society of Japan*, ed. S. Somiya and M. Doyama, Elsevier Science Bv, Amsterdam, 2006, vol. 31, no. 3, pp. 627–631.
- 16 P. Kingshott, J. Wei, D. Bagge-Ravn, N. Gadegaard and L. Gram, Covalent attachment of poly(ethylene glycol) to surfaces, critical for reducing bacterial adhesion, *Langmuir*, 2003, **19**, 6912–6921.
- 17 G. M. Harbers, K. Emoto, C. Greef, S. W. Metzger, H. N. Woodward, J. J. Mascali, *et al.* Functionalized poly(ethylene glycol)-based bioassay surface chemistry that facilitates bio-immobilization and inhibits nonspecific protein, bacterial, and mammalian cell adhesion, *Chem. Mater.*, 2007, **19**, 4405–4414.
- 18 J.-C. Yang, C. Zhao, I. F. Hsieh, S. Subramanian, L. Liu, G. Cheng, *et al.* Strong resistance of poly(ethylene glycol) based α -tyrosine polyurethanes to protein adsorption and cell adhesion, *Polym. Int.*, 2012, **61**, 616–621.
- 19 D. W. Branch, B. C. Wheeler, G. J. Brewer and D. E. Leckband, Long-term stability of grafted polyethylene glycol surfaces for use with microstamped substrates in neuronal cell culture, *Biomaterials*, 2001, **22**, 1035–1047.
- 20 A. Roosjen, J. de Vries, H. C. van der Mei, W. Norde and H. J. Busscher, Stability and effectiveness against bacterial adhesion of poly(ethylene oxide) coatings in biological fluids, *J. Biomed. Mater. Res., Part B*, 2005, **73**, 347–354.
- 21 G. Cheng, H. Xue, G. Li and S. Jiang, Integrated Antimicrobial and Nonfouling Hydrogels to Inhibit the Growth of Planktonic Bacterial Cells and Keep the Surface Clean, *Langmuir*, 2010, **26**, 10425–10428.
- 22 W. Yang, H. Xue, L. R. Carr, J. Wang and S. Jiang, Zwitterionic poly(carboxybetaine) hydrogels for glucose biosensors in complex media, *Biosens. Bioelectron.*, 2011, **26**, 2454–2459.
- 23 S. Jiang and Z. Cao, Ultralow-Fouling, Functionalizable, and Hydrolyzable. Zwitterionic Materials and Their Derivatives for Biological Applications, *Adv. Mater.*, 2010, **22**, 920–932.
- 24 Y. Chang, S.-H. Shu, Y.-J. Shih, C.-W. Chu, R.-C. Ruaan and W.-Y. Chen, Hemocompatible mixed-charge copolymer brushes of pseudozwitterionic surfaces resistant to nonspecific plasma protein fouling, *Langmuir*, 2009, **26**, 3522–3530.
- 25 W. Gao, B. Xiang, T.-T. Meng, F. Liu and X.-R. Qi, Chemotherapeutic drug delivery to cancer cells using a combination of folate targeting and tumor microenvironment-sensitive polypeptides, *Biomaterials*, 2013, **34**, 4137–4149.
- 26 X. Sun, S. Chen, J. Han and Z. Zhang, Mannosylated biodegradable polyethyleneimine for targeted DNA delivery to dendritic cells, *Int. J. Nanomed.*, 2012, **7**, 2929–2942.
- 27 Y. Wang, G. Wu, X. Li, J. Chen, Y. Wang and J. Ma, Temperature-triggered redox-degradable poly(ether urethane) nanoparticles for controlled drug delivery, *J. Mater. Chem.*, 2012, **22**, 25217–25226.

- 28 R. Bird, T. Freemont and B. R. Saunders, Tuning the properties of pH-responsive and redox sensitive hollow particles and gels using copolymer composition, *Soft Matter*, 2012, **8**, 1047–1057.
- 29 S. Carregal-Romero, M. Ochs, P. Rivera-Gil, C. Ganas, A. M. Pavlov, G. B. Sukhorukov, *et al.* NIR-light triggered delivery of macromolecules into the cytosol, *J. Controlled Release*, 2012, **159**, 120–127.
- 30 C. Zhao and J. Zheng, Synthesis and characterization of poly(*N*-hydroxyethylacrylamide) for long-term antifouling ability, *Biomacromolecules*, 2011, **12**, 4071–4079.
- 31 C. Zhao, Q. Chen, K. Patel, L. Li, X. Li, Q. Wang, *et al.* Synthesis and characterization of pH-sensitive poly(*N*-2-hydroxyethyl acrylamide)-acrylic acid (poly(HEAA/AA)) nanogels with antifouling protection for controlled release, *Soft Matter*, 2012, **8**, 7848–7857.
- 32 B. Yang, S. Y. Geng, X. M. Liu, J. T. Wang, Y. K. Chen, Y. L. Wang, *et al.* Positively charged cholesterol derivative combined with liposomes as an efficient drug delivery system, *in vitro* and *in vivo* study, *Soft Matter*, 2012, **8**, 518–525.
- 33 F. Fayazpour, B. Lucas, C. Alvarez-Lorenzo, N. N. Sanders, J. Demeester and S. C. De Smedt, Physicochemical and transfection properties of cationic hydroxyethylcellulose/DNA nanoparticles, *Biomacromolecules*, 2006, **7**, 2856–2862.
- 34 C. F. Jones, R. A. Campbell, Z. Franks, C. C. Gibson, G. Thiagarajan, A. Vieira-de-Abreu, *et al.* Cationic PAMAM Dendrimers Disrupt Key Platelet Functions, *Mol. Pharmaceutics*, 2012, **9**, 1599–1611.
- 35 E. R. Gillies, A. P. Goodwin and J. M. J. Fréchet, Acetals as pH-Sensitive Linkages for Drug Delivery, *Bioconjugate Chem.*, 2004, **15**, 1254–1263.